ELSEVIER

In vitro biodegradation of three brushite calcium phosphate cements by a macrophage cell-line

Zhidao Xia[a], Liam Michael Grover[b,1], Yizhong Huang[c], Iannis E. Adamopoulos[a],
Uwe Gbureck[d], James T. Triffitt[a], Richard M. Shelton[e], Jake E. Barralet[b,*]

[a]*Nuffield Department of Orthopaedic Surgery, The Botnar Research Centre, Institute of Muskuloskeletal Sciences,
University of Oxford, Oxford OX3 7LD, UK*
[b]*Faculty of Dentistry, McGill University, Montréal, Québec, Canada H3A 2B2*
[c]*The Department of Materials, University of Oxford, Oxford OX1 3PH, UK*
[d]*Department of Functional Materials in Medicine and Dentistry, University of Würzburg, Würzburg D-97070, Germany*
[e]*Biomaterials Unit, School of Dentistry, University of Birmingham, Birmingham B6 4NN, UK*

Abstract

Depending upon local conditions, brushite ($CaHPO_4 \cdot 2H_2O$) cements may be largely resorbed or (following hydrolysis to hydroxyapatite) remain stable in vivo. To determine which factors influence cement resorption, previous studies have investigated the solution-driven degradation of brushite cements in vitro in the absence of any cells. However, the mechanism of cell-mediated biodegradation of the brushite cement is still unknown. The aim of the current study was to observe the cell-mediated biodegradation of brushite cement formulations in vitro. The cements were aged in the presence of a murine cell line (RAW264.7), which had the potential to form osteoclasts in the presence of the receptor for nuclear factor kappa B ligand (RANKL) in vitro, independently of macrophage colony stimulating factor (M-CSF). The cytotoxicity of the cements on RAW264.7 cells and the calcium and phosphate released from materials to the culture media were analysed. Scanning electron microscopy (SEM) and focused ion beam (FIB) microscopy were used to characterise the ultrastructure of the cells. The results showed that the RAW264.7 cell line formed multinucleated TRAP positive osteoclast-like cells, capable of ruffled border formation and lacunar resorption on the brushite calcium phosphate cement in vitro. In the osteoclast-like cell cultures, ultrastuctural analysis by SEM revealed phenotypic characteristics of osteoclasts including formation of a sealing zone and ruffled border. Penetration of the surface of the cement, was demonstrated using FIB, and this showed the potential demineralising effect of the cells on the cements. This study has set up a useful model to investigate the cell-mediated cement degradation in vitro.
© 2006 Elsevier Ltd. All rights reserved.

Keywords: Brushite; Calcium phosphate cements; Biodegradation; Macrophage; Osteoclast; Focused ion beam microscopy (FIB)

1. Introduction

Although bone has the ability to repair itself following damage, extensive tissue loss due to trauma, surgical removal or disease may require the placement of a bone graft to prevent fibrous tissue in-growth and to preserve mechanical integrity. The most frequently used bone graft is autogenous tissue which is usually harvested from the iliac crest or the ribs [1]. While autografts remain the most frequently used bone grafting material, this is associated with a number of serious drawbacks including lack of availability, donor site morbidity and possible permanent gait disturbance as a result of the harvesting procedure [2]. The disadvantages associated with autografts have resulted in a large amount of research activity to find synthetic alternatives. In the past 20 years, perhaps the most frequently investigated synthetic bone grafts have been the calcium orthophosphate ceramics. One class of calcium

---

*Corresponding author. Tel.: +1 514 398 7203.

E-mail address: jake.barralet@mcgill.ca (J.E. Barralet).

[1]Present address: Chemical Engineering, University of Birmingham, Birmingham B15 2TT, UK.

orthophosphate used in bone grafting applications are the calcium phosphate cements (CPCs) [3]. They typically set following the combination of a solid component containing one or more calcium orthophosphate powders with an aqueous solution. Depending upon the pH value of the cement paste the end-product of the cement setting reaction may be either brushite (pH $\leqslant$ 4.2) [4] or hydroxyapatite (pH > 4.2) [5]. Perhaps because they are usually set at a pH value closer to the physiological environment than brushite cements, hydroxyapatite cements have been more frequently studied. However, brushite is more soluble than hydroxyapatite in physiological conditions and as a consequence has been shown to be more completely resorbed following implantation in animal models [6].

The degradation of brushite cement in vitro has been tested using phosphate-buffered saline, serum and simulated body fluid [7]. These studies have demonstrated that degradation involves erosion, fragmentation and dissolution, all of which release calcium and phosphate ions into solution. The rate at which dissolution may occur from the brushite cement is dependent upon the chemical equilibrium between dissolution and recrystallisation. Whole blood is supersaturated with respect to calcium and phosphate ions to such an extent that spontaneous precipitation of hydroxyapatite in vivo is prevented only by the presence of a number of ionic and protein crystallisation inhibitors [8]. Supersaturation of the in vivo milieu with regard to calcium and phosphate ions means that the dissolution of brushite from the cement ought to occur slowly and so cannot entirely explain the complete degradation of brushite cements in vivo. A recent study has reported that in vivo brushite cement degradation is aided by macrophages which phagocytose cement particles [9].

Previous studies have investigated the solution-driven degradation of the brushite cements in vitro in the absence of any of the cells encountered in vivo [7]. The aim of the current study was to observe the cell-mediated biodegradation of three different brushite cement formulations in vitro. The selected cements set to form matrices consisting of different proportions of brushite and either β-tricalcium phosphate (β-TCP) or nanocrystalline hydroxyapatite. To investigate the potential roles of macrophages and osteoclasts in cement degradation, RAW264.7, a murine monocyte/macrophage cell line, which has the potential to form osteoclasts in vitro independently of macrophage colony stimulating factor (M-CSF) was selected for the study. The cytotoxicity of the cements on RAW264.7 cells, the calcium and phosphate released from materials and ultrastructure of the cells on materials were also analysed.

2. Materials and methods

2.1. Specimen preparation

Three different brushite cements were examined in this study. Two of the cements set following the combination of either β-TCP (Plasma-Biotal, Derbyshire, UK) or nanocrystalline hydroxyapatite, precipitated in accordance with the method reported previously [10], with orthophosphoric acid solution (Table 1). The third cement set following the combination of β-TCP (Plasma-Biotal, Derbyshire, UK) with an orthophosphoric acid/pyrophosphoric acid blend (Rhodia, West-Midlands, UK) and double-distilled water. All cements were mixed to a powder to liquid ratio of 1.75 g/mL. The cement formulations and the abbreviations used throughout the paper are listed in Table 1. To form cylindrical specimens of diameter 6 mm and height 12 mm, the cement pastes were cast into a PTFE split mould and once set were removed from the mould before storage for 24 h at $37 \pm 1\,^{\circ}C$ and 100% relative humidity. The set specimens were sectioned by using a low speed diamond saw (Isomet, Buehler, IL, USA) at a speed of 100 revolutions per minute using DP blue (Struers, Glasgow, UK) to lubricate the blade. The resulting nominally identical discs of height 2 mm were then sterilised using ethylene oxide. The cement discs were washed in 25 mL 100 mM phosphate buffered saline (PBS; Sigma-Aldrich, Gillingham, UK) for 1 h and were stored in PBS for 12 h. The discs were washed in α-MEM (Gibco BRL, Paisley, UK) twice for 1 h and were stored in α-MEM for an additional 24 h. A single cement disc was placed in each well of a 96-well tissue culture plate (Fahrenheit, Milton-Keynes, UK).

2.2. Cell culture

The RAW264.7 murine macrophage cells were recovered from stock as previously reported [11] and cultured in 10% foetal calf serum (FCS) (MB Meldrum Ltd., Buckinghamshire, UK) α-MEM. Cells were removed from culture substrates for further experiments using a disposable cell scraper. The seeding density for RAW264.7 cells was 4×10^5 cells/cm^2. The cells were fed using 10% FCS α-MEM supplement with 25 ng/mL M-CSF (R&D Systems Europe Ltd., Oxfordshire, UK) to maintain their macrophage phenotype, or with 10 ng/mL receptor for nuclear factor kappa B ligand (RANKL) (Peprotech Europe Ltd., Oxfordshire, UK) to induce osteoclast differentiation. Culture medium was replaced on days 1, 4, 7, 11 and 14. Culture medium was collected and frozen in sealed vials at $-20\,^{\circ}C$ before replenishment on days 1, 7 and 14. The frozen medium was thawed for 6 h at ambient temperature ($24 \pm 1\,^{\circ}C$) for measurement of pH and calcium and phosphorus concentrations. Cells cultured on cement were analysed on days 7 and 14 using the LIVE/DEAD assay (Molecular Probe, Leiden, The Netherland).

Table 1
The formulations, abbreviations and the proportion of the hardened cement contributed by brushite for the three brushite cement formulations used in this study

Cement	Nature of solid component	Acid component	Additives	Proportion of brushite in set cement (wt%)
BR	β-TCP	2 M H_3PO_4	50 mM trisodium citrate	34
NA	Nanocrystalline hydroxyapatite	3.5 M H_3PO_4	None	70
NO	β-TCP	1.5 M $H_4P_2O_7$ 2.7 M H_3PO_4	None	84

2.3. Media characterisation

The pH value of the culture medium at each time-point was determined using a pH meter (420, Mettler-Toledo, Leicestershire, UK) from the average of three measurements. An inductively coupled mass spectrometer (Varian, Darmstadt, Germany) was used to determine the Ca^{2+} and PO_4^{3-} contents of the culture media. Following dilution to 1:1000 using de-ionised water about 15 mL of this solution was transferred to a polyethylene tube for measurement. To determine the precise Ca^{2+} and PO_4^{3-} ion concentrations the diluted culture media were compared with standard solutions containing Ca^{2+} and PO_4^{3-} at concentrations of 0, 10, 100 and 1000 parts per billion.

2.4. Tartrate-resistant acid phosphatase (TRAP) staining

TRAP staining was used to identify whether the RAW264.7 macrophages differentiated to form osteoclasts following the addition of RANKL to the culture. Briefly, cells were fixed using 10% formaldehyde for 10 min and then using a 1:1 volume mixture of ethanol and acetone for 1 min. The cells were washed once using 100 mM PBS. Fast-red salt (Sigma-Aldrich, Gillingham, UK) was then added to TRAP solution (containing 59.3 M sodium tartrate, 165.7 mM sodium acetate, and 0.56 mg/mL naphthol AS-MX phosphate) and the cells were incubated in the resultant solution for 5 min at 25 °C.

2.5. Cell viability assay

On day 7, cells were washed twice with PBS to remove foetal calf serum in culture medium which would interfere with the staining procedures to assess the cell viability of RAW264.7 cells. Samples were stained using a LIVE/DEAD stain kit (Molecular Probes, Leiden, The Netherland). The kit contained two fluorescent dyes: calcein to stain living cells green and ethidium homodimer-1 (Ethd-1) to stain damaged or dead cells red. Samples were stained using 4 μM calcein and 2 μM Ethd-1 (final concentration) in PBS for 30 min at 37 ± 1 °C. Samples were rinsed twice using PBS to remove any dye and fixed either in 4% formaldehyde (Sigma-Aldrich, Dorset, UK) or 4% glutaraldehyde (Sigma-Aldrich, Dorset, UK) in 100 mM PBS at 4 ± 1 °C to prevent cell detachment from the surface of the cement. Samples were washed again in PBS to remove the fixative before being observed using fluorescence microscopy. Images were captured using a colour video camera (JVC 3-CCD, KY-F55B, Yokohama, Japan) at 100 × magnification using the Optimas 5.1 software (Optimas Corp., Seattle, USA). For each sample, three images were captured. Images were opened in Adobe photoshop 6.0 (San Jose, CA, USA) and each image (1.18 mm^2) was divided into 50 squares using a grid. Live and dead cells were counted in five squares to estimate the cell numbers in an image. Three indices were selected for analysis as follows:

$$\text{Number of cells per disc} = \left(\sum_{i=1}^{3} Ni \right) / 3 / CA, \qquad (1)$$

$$\text{Total cell number per disc} = (\text{Live cells (green) per disc} + \text{Dead cells (red) per disc}), \qquad (2)$$

Dead cell ratio (%)

$$= \left(\frac{\text{Average number of dead cells (red)}}{\text{Total number of cells (red and green)}} \right) \times 100, \qquad (3)$$

where N is the number of cells per image, C is the calibrated area of an image at given magnification, in this case $C = 1.18\,mm^2$, and A is the surface area of the cement disc (28.26 mm^2).

2.6. Scanning electron microscopy (SEM) and focused ion beam (FIB) microscopy

The cements with cells were fixed in 4% glutaraldehyde, 100 mM PBS and dehydrated using a graded series of ethanol up to absolute, which was finally substituted with hexamethyldisilazane (Sigma-Aldrich Company Ltd., Dorset, UK) and left to dry in ambient conditions overnight. The samples were mounted on stubs and sputter-coated with gold prior to examination using a JEOL JSM 5300 scanning electron microscope (JEOL, Tokyo, Japan). A focused ion beam microscope [12] (FIB 200TEM, FEI UK Ltd., Cambridge, UK) was used to examine the ultrastructure of the cells. When a target cell was selected, a rectangle covering the desired surface was chosen. Ion milling was initiated with a beam current of 1000–3000 picoamperes (pA) on the chosen area to etch a given depth (d) on the surface. The image was revealed and recorded at a sample tilt of 45°, in which a beam current of 10 pA was used in order to minimise the possible damage during ion beam scanning.

2.7. Statistical analysis

Multiple comparisons of the data were performed using a one-way analysis of variance (ANOVA) within a statistical analysis package (GraphPad InStat®, v.3.06 for Windows, San-Diego, USA). A Tukey multiple range post hoc test was used to compare paired groups of data. Statistical tests were performed at a 95% significance level ($p < 0.05$).

3. Results

3.1. Cement cytotoxicity

The morphology of RAW264.7 cells are shown in Fig. 1. RAW264.7 cells were 6–10 μm in diameter (Fig. 1a). By RANKL treatment, osteoclast-like multinuclear giant cells were observed (Fig. 1b). RANKL treated cultures of RAW264.7 cells contained TRAP$^+$ cells (Fig. 1c), whereas no TRAP$^+$ cells were noted in control cultures. The RAW264.7 cells on the cements after LIVE/DEAD

Fig. 1. RAW264.7 cells on glass coverslips, images captured using light microscopy: (a) control RAW264.7 cells; (b) osteoclast-like cells formed in vitro in RANKL treated cultures; and (c) TRAP positive staining of the osteoclast-like cells in RANKL treated cultures.

fluorescent staining are shown in supplement Fig. 1. The total cell numbers on the three cements are shown in Fig. 2. In control cultures (RANKL-) cell numbers on the NA cement declined significantly from day 7 to day 14 ($p < 0.01$), and the cell number on this cement was significantly lower than those on either the BR or NO cements ($p < 0.01$) at any time-point. There was no significant difference between the cell numbers on the BR and NO cements at any time-point (Fig. 2A). In RANKL treated cultures, the total cell numbers on the NA, BR and NO cements all declined significantly between 7 and 14 days of culture ($p < 0.001$, <0.001 and <0.01, respectively). Of the three cements studied, in the presence of RANKL the total cell number on the NA cement after both day 7 and 14 was significantly ($p < 0.001$) lower than that on either the BR or NO cement. There was no significant difference in cell numbers on the BR and NO cements cultured in the presence of RANKL after either 7 or 14 days of culture (Fig. 2B).
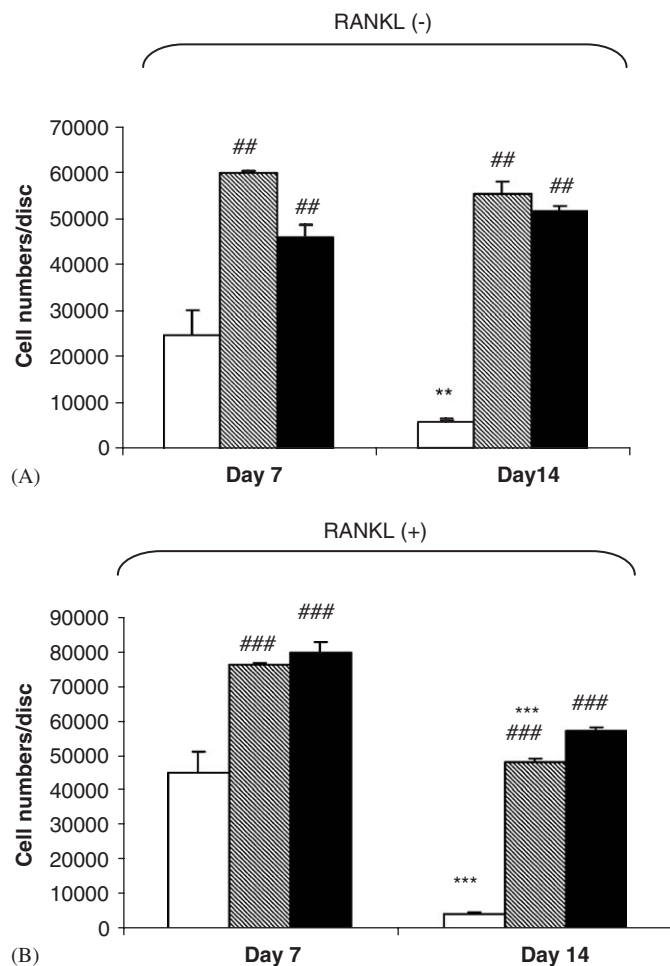

Fig. 2. The total cell number on the NA (□), BR (▨) and NO (■) cement discs after 7 and 14 days of culture in (A) the absence and (B) presence of RANKL (*, ***, Comparison with the same materials at day 7 and day 14, $p < 0.05$ and <0.001, respectively. ##, ###, comparison with NA at the same time point, $p < 0.01$, <0.001, respectively).
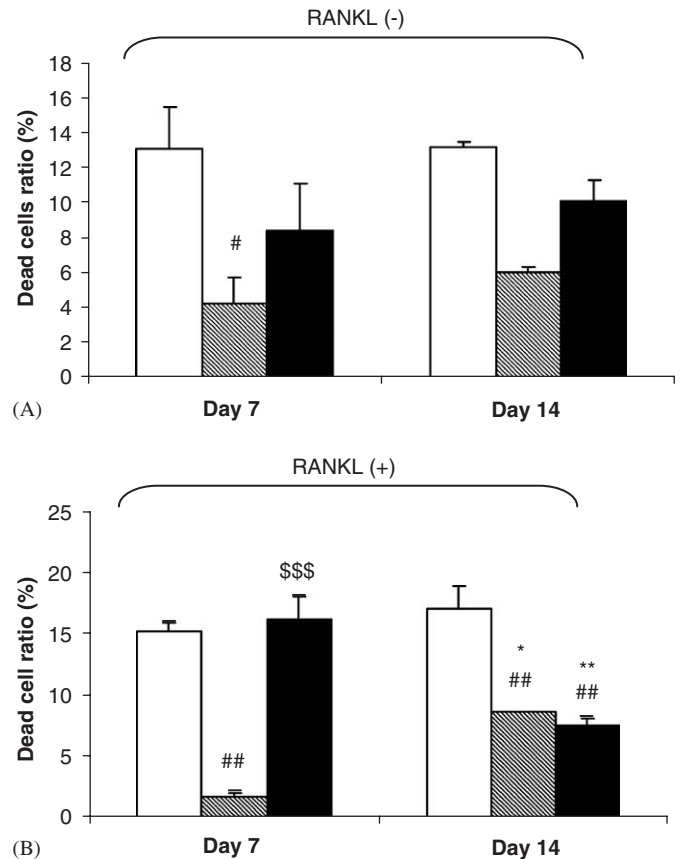

Fig. 3. The dead/live cell ratios of RAW264.7 cells cultured on the NA (□), BR(▨) and NO (■) cements for 7 and 14 days in (A) the absence of RANKL and (B) the presence of RANKL (*, **, comparison with the same materials at day 7 and day 14, $p < 0.05$ and <0.01, respectively. ♯, ♯♯, comparison with NA at the same time point, $p < 0.05$ and <0.01, respectively. $$$, comparison with BR at the same time point, $p < 0.001$).

The dead cell ratio, reflecting the cytotoxicity of the cements, is shown in Fig. 3. In all control cultures (RANKL-), except for the BR cement at day 7 which showed a lower dead cell ratio than the NA cement, there were no significant differences between day 7 and day 14 and between cements in all the three groups (Fig. 3A). In RANKL treated cultures the dead cell ratio on the NA cement remained at the same level as seen at day 7, whereas there was an increase on the BR cement ($p < 0.5$) and a decrease on the NO cement ($p < 0.01$).

3.2. Analysis of culture media

The PO_4^{3-} concentrations in the culture media are shown in Table 2. PO_4^{3-} in the NA group control cultures had increased by 4 times at day 7 ($p < 0.001$), and then halved by day 14 ($p > 0.05$). There was an increase in PO_4^{3-} in the BR group at day 14 ($p < 0.05$) compared with day 1 and day 7 but there was no significant change in the NO group at three time points. In RANKL treated cultures, there was also a dramatic increase of PO_4^{3-} at day 7 in the NA group. There was no significant change of PO_4^{3-} in the BR group at all time points, but there were decreases of PO_4^{3-} in NA

Table 2
The measured pH values and calcium and phosphorous concentrations of the minimal essential medium after 1, 7 and 14 days of culture on NA, BR and NO cement in the presence and absence of RANKL (standard deviations given in brackets)

Cement	Culture RANKL +/−	1 day			7 days			14 days		
		pH	Ca conc. (ppm)	P conc. (ppm)	pH	Ca conc. (ppm)	P conc. (ppm)	pH	Ca conc. (ppm)	P conc. (ppm)
NA	−	6.35 (0.03)	26 (10)	414 (71)	6.45 (0.02)	259 (68)	2072 (46)	6.30 (0.05)	191 (149)	912 (242)
	+	6.40 (0.04)	40 (3)	554 (24)	6.35 (0.03)	206 (64)	2332 (205)	6.11 (0.04)	0 (0)	109 (3)
BR	−	6.75 (0.02)	96 (13)	138 (1)	6.95 (0.04)	176 (88)	116 (27)	7.10 (0.04)	283 (95)	711 (33)
	+	6.8 (0.03)	163 (37)	158 (23)	6.75 (0.04)	606 (184)	221 (42)	7.00 (0.05)	9 (1)	41 (1)
NO	−	6.27 (0.05)	98 (31)	371 (47)	6.93 (0.03)	456 (93)	527 (162)	7.25 (0.03)	607 (72)	324 (26)
	+	6.23 (0.04)	188 (139)	506 (57)	6.65 (0.02)	224 (121)	431 (84)	7.10 (0.03)	48 (40)	0 (0)

and NO groups ($p < 0.01$) at day 14 compared with day 1 ($p < 0.01$). The Ca^{2+} concentrations in culture media are shown in Table 2. In all control cultures (RANKL-), the average concentration of Ca^{2+} in media increased more than threefold at day 7 and day 14 compared with day 1; however, only in the NO group at day 14 the difference was statistically significant compared with day 1 ($p < 0.01$) and the NA group at day 14 ($p < 0.01$). The dramatic differences in RANKL treated cultures in the three groups were the decrease in average Ca^{2+} concentration at day 14 however the decreases were not significant compared with day 1.

After one day of culture the NO cement caused the pH of the culture medium to drop to 6.27 ± 0.05 in control cultures and 6.23 ± 0.04 (Table 2) in RANKL treated cultures. Of the cements studied the BR cement reduced the pH of the culture medium the least (6.75 ± 0.02) in the absence of RANKL and 6.80 ± 0.03 in the presence of RANKL. With time the pH of the culture media in which the BR and NO cements were immersed increased towards pH 7–7.25, however, in the case of the NA cement the culture medium reached a pH value minimum of 6.30 ± 0.05 and 6.11 ± 0.04 after 14 days of culture.

3.3. SEM and FIB microscopy

Scanning electron micrographs of the RAW264.7 in control cultures on the NO cement are shown in Fig. 4. RAW264.7 cells were 5–10 μm diameter with fine cell processes and surface folds (Fig. 4a–c). Morphologically there were two different types of giant cells: (a) well-developed giant cells of 20–30 μm in diameter, with a few long (10–15 μm) cell processes and abundant surface folds (Fig. 4a); and (b) those formed by aggregation of RAW264.7 cells with very short and fine cell processes (Fig. 4b). A number of dead giant cells were evident as the giant cells became fragmentary with crystal-like structures formed inside cells (Fig. 4d).

By evenly milling a thin layer from the chosen area of dead giant cells on the cements (Fig. 5a and b) using FIB

microscopy, no phagocytosed particles were observed. However, in situ cross-sections of selected giant cells showed that the cell processes had penetrated deeply into the surface of the cement and had engulfed cement particles (Fig. 5c and d). A gap between cell and cement particles was evident (Fig. 5e).

In RANKL treated cultures, less than 30% of RAW264.7 cells differentiated into osteoclast-like cells and these cells were TRAP positive. These giant cells were of diameter 30–50 μm with abundant microfilaments on the cell surface (Fig. 6a and b). The well-developed osteoclast-like cells formed an apparent sealing-zone where the outer aspect of the cell membrane contacted the cement substratum (Fig. 6b). The cell morphologies in RANKL treated cultures were of non-differentiated cells (Fig. 6c), differentiated osteoclast-like cells (Fig. 6d), apoptotic osteoclast-like cells (Fig. 6e) and dead osteoclast-like cells with crystal formation (Fig. 6f).

The FIB milling analysis (Fig. 7a) confirmed that the cell processes of the osteoclast-like cells penetrated deeply into the cements (Fig. 7b–d). At the cell–cement interface, the cell membranes of osteoclast-like cells formed ruffled-borders and extended into the gaps between the cement particles (Fig. 7e and f), and there were abundant vesicles in the cytoplasm (Fig. 7c, e and f).

4. Discussion

Although brushite cements were originally reported almost 20 years ago [13] the literature contains few references to the cellular reactions to these cements in vitro. One possible reason for this is that the cements set by an acid/base reaction, which reduces the pH value of the cement mix to as low as 3 [4]. As cell culture medium has a relatively low inherent buffering capacity such pH alterations are likely to have an acute toxic effect on the cells. Indeed in this study although the cement samples were extensively washed in phosphate-buffered saline and α-MEM prior to culture, the medium had a pH of
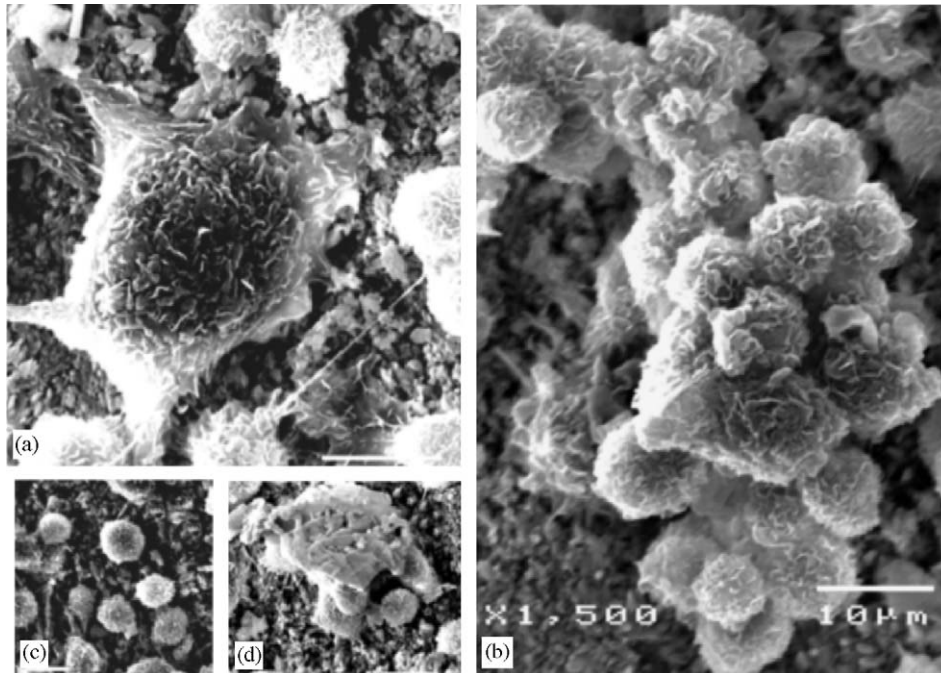
Fig. 4. Scanning electron micrographs of macrophages on NO cement: (a) well differentiated giant macrophage at 14 days. Notice the cell size of giant cells compared with the undifferentiated cells around; (b) the fusion of RAW264.7 cells to form giant cells at 14 days; (c) undifferentiated RAW264.7 cells at day 7; and (d) dead giant cells at 14 days showing cell fragmentation with crystal-like structures within cells. Bar = 10 μm.
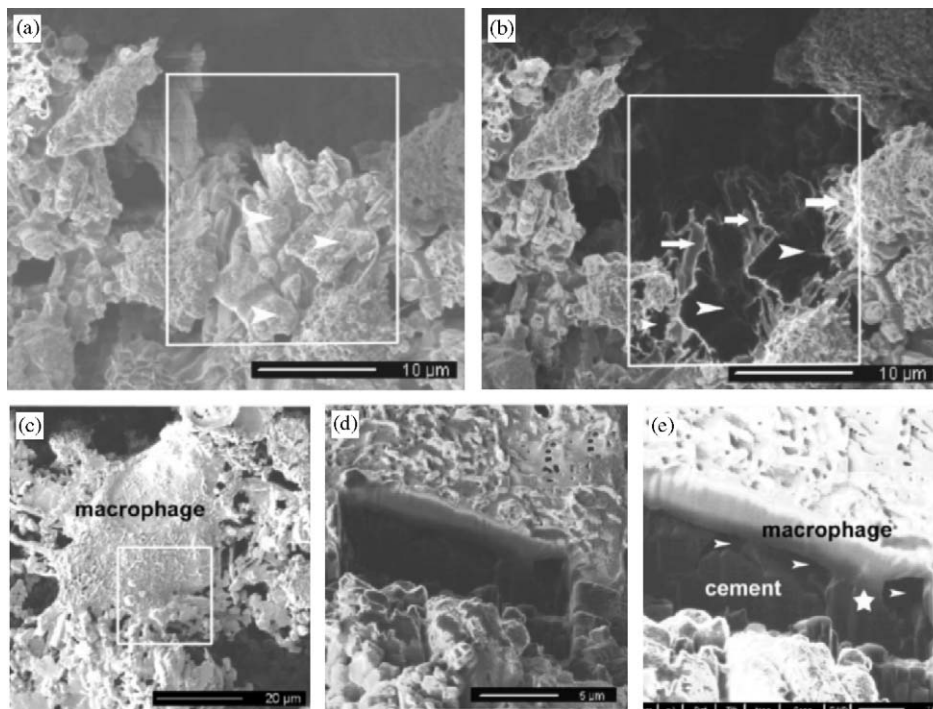

Fig. 5. Focussed ion beam electron images showing: (a) a giant cell that showed cell fragmentation with crystal-like structures within the cell was chosen for milling to demonstrate internal structure; (b) the milled giant cell, except for cell membranes (arrows with tail), the crystal-like structure (arrow without tail) was actually empty; (c) an area of interest on a live giant cell was chosen for milling; (d) after milling the giant cell was tilted by 45° exposing the interface between the macrophage and the cement; and (e) a cell process of the giant macrophage had penetrated the cement (☆). The gaps between cells and cement were visible (arrows without tail).

6.23 ± 0.04 (Table 2) after the first day in culture. This pH rose subsequently after 7 and 14 days as a consequence of further medium changes and replenishment. Despite the low pH of brushite cements immediately after setting there have been a number of in vivo studies which have reported favourable host responses after implantation [14,15]
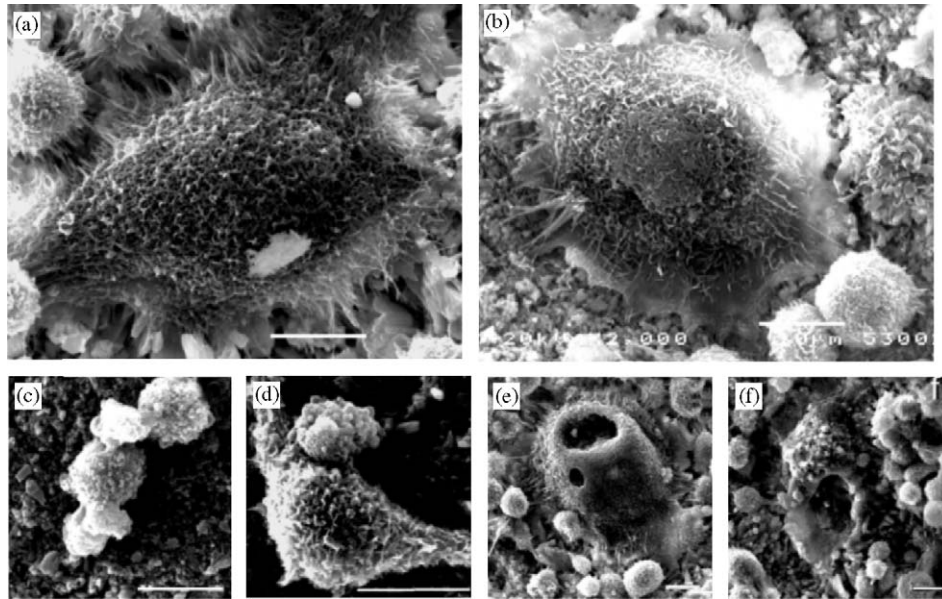
Fig. 6. Scanning electron micrographs of osteoclast-like cells on NO cement: (a) 7 days after seeding; (b) well-developed osteoclast-like cell 14 days after seeding. Notice the sealing zone formed by cell membrane along the border of the cell and the cell size compared with nearby undifferentiated cells; (c) undifferentiated RAW264.7 cells 7 days after seeding; (d) differentiated cells 7 days after seeding; (e) an apoptotic osteoclast-like cell at 7 days after seeding. Notice the damaged cell membrane; and (f) a dead osteoclast-like cell 14 days after seeding, notice the crystals formed on the dead cell. Bar = 10 μm.

demonstrating the functional buffering capacity of the in vivo milieu.

The same mechanism of decomposition is presumed for CPCs [16] as for calcium phosphate ceramics [17], although the cell type involved in their breakdown varies according to the type of cement. CPCs that are resorbed relatively quickly are removed by macrophages and giant cells, whilst the more slowly resorbed CPCs are degraded by osteoclast-like cells [18]. Our study demonstrates that RAW264.7 cells in control and RANKL treated cultures formed macrophages and multinucleated giant cells on the cements. The increase in calcium concentrations in the RANKL(−) groups evidently showed the biodegradation of the cements. There was no evidence in the current study to show whether or not the cement particles were phagocytosed by small-sized single nuclear macrophages. By evenly milling a thin layer from an area of dead giant cells present on the cements, it was demonstrated that there were no cement particles within the dead multinuclear giant cells (Fig. 5a and b). There was not sufficient evidence to show phagocytosis of the giant cells in the current study, however, cell processes were observed to have penetrated deeply into the surface of the cements (Fig. 5c and d). Mouse macrophages and giant cells are capable of phagocytosing biomaterial particles less than the size of the cells [19,20]. For biodegradation to be mediated by phagocytosis of particles from the cement surface, particles should have been found within the cells. However, this was not the case and any biodegradation of the cement in the current study was likely to be due to extracellular dissolution rather than phagocytosis.

Osteoclasts have been shown to form resorption lacunae on the surface of CPCs [21] and the present study has demonstrated the presence of multinucleated TRAP positive osteoclast-like cells, capable of ruffled border formation and lacunar resorption on the surface of the brushite cement in RANKL treated cultures. The degradation of brushite by osteoclasts may be expected to cause a local increase in calcium concentration. However, in this study this was not the case as in the presence of RANKL the activity of osteoclast-like cells did not result in increases of Ca and P concentration in the culture medium over and above that seen in the absence of RANKL. On the contrary, a trend of decreases in Ca and P (although not significant for Ca concentrations) was observed in the RANKL treated group although the cause of this trend is unknown. Possible reasons may be: (1) 30 ng/mL RANKL only stimulated less than 30% of RAW264.7 cells to differentiate to osteoclast-like cells; (2) the life span of osteoclast-like cells differentiated from RAW264.7 cells were 11–14 days so after 14 days most osteoclastic cells had undergone apoptosis. The decrease in total cell number in RANKL(+) samples at day 14 reflected this cell death and was also shown by the SEM observations; (3) there was recrystallisation of mineral in the cement matrix and in apoptotic osteoclast-like cells. The minerals accumulated in apoptotic osteoclasts before transport out may become a source of Ca^{2+} to trigger remineralisation, as seen in Fig. 6. The variable calcium and phosphate contents of the media at various time points may reflect this crystal deposition and the lowest values seen at 14 days in the RANKL treated cultures signify greatest
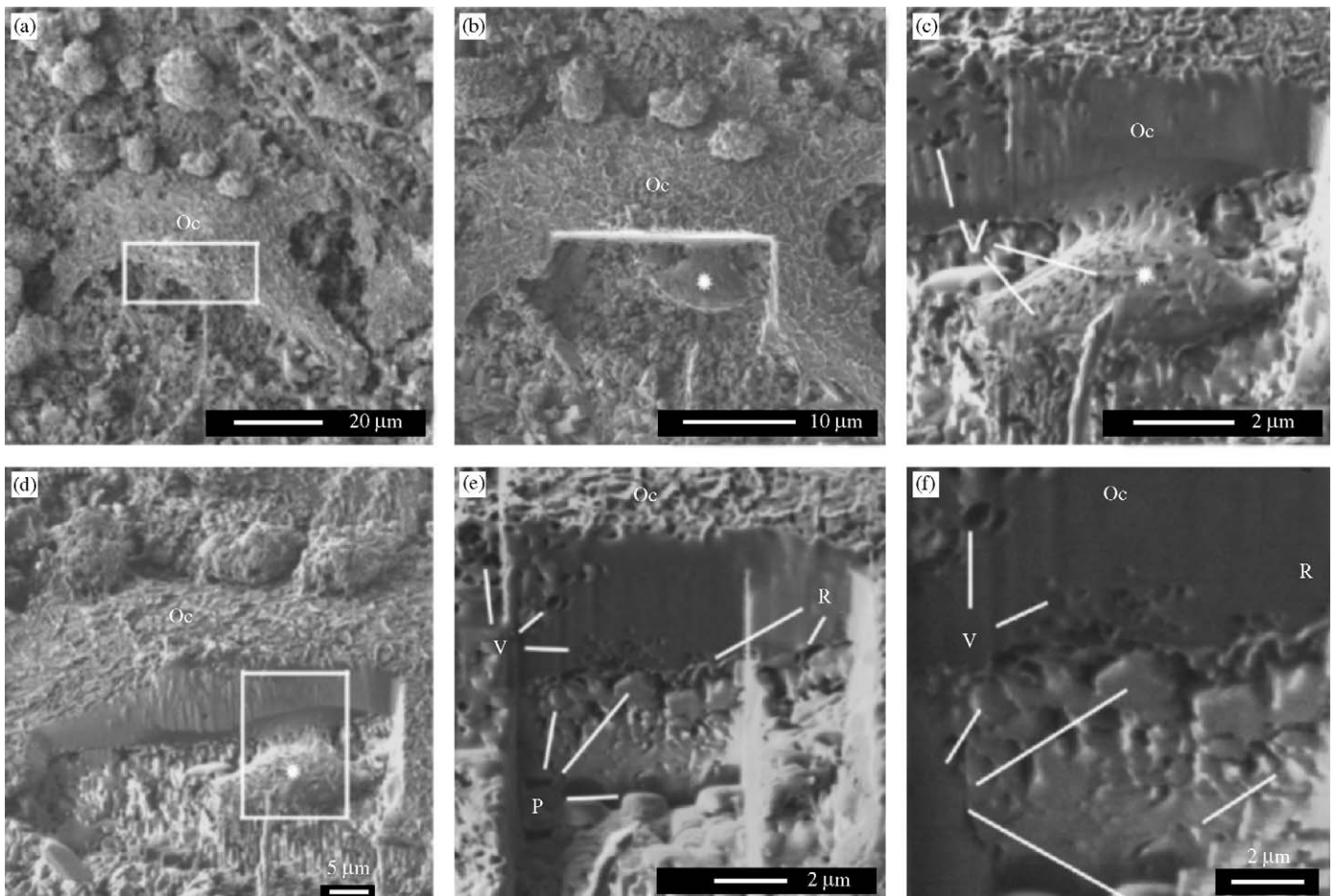
Fig. 7. Focussed ion beam electron images showing the interface between an osteoclast-like cell and NO cement: (a) shows the area on an osteoclast-like cell chosen for milling; (b) the chosen area after milling, the part of cell labelled with a white star penetrating into the cement; (c) the sample tilted by 45° to highlight the cell penetration and the cell part and cell–material interface; (d) an additional area of interest selected for milling; (e) following milling of (c) the remaining cell organelles were removed and the interface between cell and material was exposed; and (f) a higher magnification of (e) to highlight the ruffled-border of the cells. Oc, osteoclast-like cells; V, vesicles within the osteoclast-like cells; P, cement particles; and R, the ruffled border of the osteoclast-like cells.

precipitation at this time point resulting in the lowest $Ca \times P$ products.

It has been reported that osteoclasts may not resorb brushite cements as rapidly as hydroxyapatite cements because at a pH of 3.9–4.2, brushite is actually less soluble than hydroxyapatite [22]. Osteoclast mediated resorption, therefore, may be expected to occur more slowly on brushite cement than on hydroxyapatite cements. With time, the brushite in the cement may hydrolyse to form hydroxyapatite, as this change occurs it would be expected that osteoclasts could play a more dominant role in material degradation.

The hydrolysis reaction (Eq. (4)) is generally considered to be undesirable since the formation of hydroxyapatite in the cement matrix can result in a reduction in the rate at which the cement may be resorbed [9].

$$10CaHPO_4 \cdot 2H_2O$$
$$\rightarrow Ca_{10}(PO_4)_6OH_2 + 4HPO_4^{2-} + 6H^+ + H_2O. \qquad (4)$$
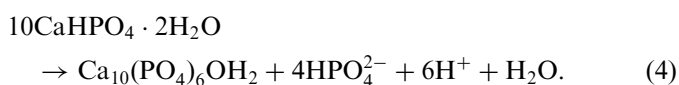
As Eq. (4) illustrates, the hydrolysis of brushite (molar calcium to phosphorous ratio = 1) to stoichiometric hydroxyapatite (theoretical molar calcium to phosphorous ratio = 1.67) results in the liberation of acid phosphate and hydrogen ions. It may be that the marked increase in phosphorous concentration (Table 2) and accompanying reduction in pH of the medium in which the NA brushite cement was aged (Table 2) may be attributed to the hydrolysis of the brushite component of the cement to hydroxyapatite.

It is generally accepted that cement resorption occurs through extracellular liquid dissolution with cement disintegration and particle formation, and phagocytosis of the cement particles by macrophages [9]. The phagocytosis of cement particles was not supported in the current study using RAW264.7 cells. However, by using focused ion beam milling, the multinuclear giant cells were found to partly engulf the cements via cell pseudopodia penetrating deeply into the cements to form a sealed compartment. In addition, the osteoclast-like cells formed a sealing-zone and

ruffled border and resorption lacunae-like structures. This suggests that extracellular degradation of cement by multinuclear giant cells may also play a role in the cement resorption.

5. Conclusion

In conclusion, the RAW264.7 cell line formed macrophage/multinucleated giant cells and osteoclast-like cells on the brushite CPCs in vitro. The significant release of calcium in the NO cement showed biodegradation of the cement in the presence of macrophage/multinucleated giant cells. Although calcium levels were not elevated in the culture media from the osteoclast-like cell cultures, ultra-structural analysis by SEM revealed phenotypic characteristics of osteoclasts including formation of a sealing zone and ruffled border. Penetration deep inside the surface of the cements showed the potential for their demineralisation by cellular activities. This study has developed a useful model to investigate the cell-mediated cement degradation in vitro and demonstrates the value of focused ion beam microscopy in investigation of cell–biomaterial interactions.

Acknowledgement

Appendix A. Supplementary material

Supplementary data associated with this article can be found in the online version at: doi:10.1016/j.biomaterials. 2006.04.030.

References

[1] Goulet JA, Senunas LE, DeSilva GL, Greenfield ML. Autogenous iliac crest bone graft. Complications and functional assessment. Clin Orthop Relat Res 1997;339:76–81.
[2] Fowler BL, Dall BE, Rowe DE. Complications associated with harvesting autogenous iliac bone graft. Am J Orthop 1995;24:895–903.
[3] Jansen J, Ooms E, Verdonschot N, Wolke J. Injectable calcium phosphate cement for bone repair and implant fixation. Orthop Clin North Am 2005;361:89–95.
[4] Bohner M, Van Landuyt P, Merkle HP, Lemaitre J. Composition effects on the pH of a hydraulic calcium phosphate cement. J Mater Sci-Mater Med 1997;8:675–81.
[5] Brown PW, Chow LC. A calcium phosphate water setting cement. Cements research progress. In: Proceedings of the American Ceramics Society, 1986. p. 352–79.
[6] Klein CP, de Groot K, Driessen AA, van der Lubbe HB. Interaction of biodegradable beta-whitlockite ceramics with bone tissue: an in vivo study. Biomaterials 1985;6:189–92.
[7] Grover LM, Knowles JC, Fleming GJP, Barralet JE. In vitro ageing of brushite calcium phosphate cement. Biomaterials 2003;24:4133–41.
[8] Terkeltaub RA, Santoro DA, Mandel G, Mandel N. Serum and plasma inhibit neutrophil stimulation by hydroxyapatite crystals. Evidence that serum alpha 2-HS glycoprotein is a potent and specific crystal-bound inhibitor. Arthritis Rheum 1988;31:1081–9.
[9] Theiss F, Apelt D, Brand B, Kutter A, Zlinszky K, Bohner M, et al. Biocompatibility and resorption of a brushite calcium phosphate cement. Biomaterials 2005;26:4383–94.
[10] Barralet JE, Lilley KJ, Grover LM, Farrar DF, Ansell C, Gbureck U. Cements from nanocrystalline hydroxyapatite. J Mater Sci-Mater Med 2004;15:407–11.
[11] Itonaga I, Sabokbar A, Sun SG, Kudo O, Danks L, Ferguson D, et al. Transforming growth factor-beta induces osteoclast formation in the absence of RANKL. Bone 2004;34:57–64.
[12] Huang YZ, Lozano-Perez S, Langford RM, Titchmarsh JM, Jenkins ML. Preparation of transmission electron microscopy cross-section specimens of crack tips using focused ion beam milling. J Microsc 2002;207:129–36.
[13] Lemaitre J, Mirtchi A, Mortier A. Calcium phosphate cements for medical use: state of the art and perspectives of development. Silic Ind 1987;10:141–6.
[14] Frayssinet P, Gineste L, Conte P, Fages J, Rouquet N. Short-term implantation effects of a DCPD-based calcium phosphate cement. Biomaterials 1998;19:971–7.
[15] Constantz BR, Barr BM, Ison IC, Fulmer MT, Baker J, McKinney L, et al. Histological, chemical, and crystallographic analysis of four calcium phosphate cements in different rabbit osseous sites. J Biomed Mater Res 1998;43:451–61.
[16] Jarcho M. Calcium phosphate ceramics as hard tissue prosthetics. Clin Orthop Relat Res 1981;157:259–78.
[17] Damien CJ, Parsons JR. Bone graft and bone graft substitutes: a review of current technology and applications. J Appl Biomater 1991;2:187–208.
[18] Ooms EM, Wolke JG, van der Waerden JP, Jansen JA. Trebecular bone response to injectable calcium phosphate (Ca-P) cement. J Biomed Mater Res 2002;61:9–18.
[19] Xia ZD, Zhu TB, Du JY, Zheng QX, Wang L, Li SP, et al. Macrophages in degradation of collagen/hydroxylapatite(CHA), beta-tricalcium phosphate ceramics (TCP) artificial bone graft. An in vivo study. Chin Med J (England) 1994;107:845–9.
[20] Lam KH, Schakenraad JM, Esselbrugge H, Feijen J, Nieuwenhuis P. The effect of phagocytosis of poly(L-lactic acid) fragments on cellular morphology and viability. J Biomed Mater Res 1993;27:1569–77.
[21] Schilling AF, Linhart W, Filke S, Gebauer M, Schinke T, Rueger JM, et al. Resorbability of bone substitute biomaterials by human osteoclasts. Biomaterials 2004;25:3963–72.
[22] Tas AC, Bhaduri SB. Chemical processing of $CaHPO_4 \cdot 2H_2O$: its conversion to hydroxyapatite. J Am Ceram Soc 2004;87:2195–200.